A NEW APPROACH TO THE UNSUPERVISED DETECTION AND CLASSIFICATION OF THE SPLICED YARN JOINT

Khaled Issa and Hiroshi Nagahashi

Imaging Science and Engineering Laboratory, Tokyo Institute of Technology, Japan

Abstract:

This paper presents an automatic vision-based system for unsupervised detection and classification of spliced yarn joints. In the splice detection process, a competitive learning method based on an LBG algorithm is used. In the splice classification process, a dynamic time warping (DTW) algorithm is used to classify the extracted splice joint into one of three categories, based on the degree of similarity between the spliced joint and the non-spliced remaining part of the same yarn. The use of DTW in the classification makes the proposed method adaptable to different types of yarns. Consequently, this method might be universally applicable for the classification of all spliced yarn joints. The proposed method has been evaluated using three types of experiments, yielding a promising result.

Keywords:

Spliced yarn joint, Visual Inspection, VQ, DTW

1. Introduction

During the last few years, the textile industry throughout the world has been under extreme pressure to produce higher quality yarns and fabrics, owing to the increased awareness of consumers with regard to product qualities as well as severe global competition. The emphasis on ring-spun yarns and high-quality casual wear now demands the highest possible yarn and fabric qualities.

An important aspect of the fiber-to-yarn production process is the quality of the resulting yarn, which should obviously have optimum product characteristics and minimum faults, such as thins, thick, neps, etc. Weak places occurring in the yarn caused by the narrowing of yarn sections should be eliminated to avoid the danger of breakages during weaving or knitting operations. The process of removing such objectionable faults is called yarn clearing. Following removal of the faults both yarn ends must be joined together by a splicing operation. The splicing consists of untwisting the yarn ends to achieve a near parallel arrangement of fibers and later re-twisting two yarn ends together using air blast.

The correct splicing of broken yarn ends depends on many factors, but most important one is how the yarn ends are prepared [1,2,3]. However, obtaining an 'ideal' joint is practically impossible. The choice of the most favorable settings, i.e. the best technological parameters of a splicing device, is the task of engineers possessing specific knowledge of the subject.

The two important characteristics of a splice joint are appearance and physical properties. Although the physical properties of the joint can be assessed by methods like load-elongation, work of rupture, increase in diameter and evaluation of its performance in the subsequent process [4], the assessment of the appearance of the splice joint is carried out visually, accompanied by many disadvantages because it is slow and subjective and the visual assessment by humans is time consuming and cost intensive. Moreover, due to the stress of the task, human inspection does not achieve a high degree of accuracy. Thus, it became necessary to find alternative methods which could eliminate all these drawbacks.

<u>Assessment of the spliced joint appearance</u>

Analysis of the longitudinal and transverse studies revealed that the structure of the splice comprises three regions, as shown in Figure 1:

1. Wrapping: the tail end of each yarn strands and terminates with a few fibers. The tail ends make a good wrapping of several turns and thus prevent flaying of the splice. The fibers of the twisting yarn embrace the body of the yarn and thus act as a belt, Figure 1(d).

2. Twisting: the two yarn ends comprising the splice are twisted around the body of the yarn, each yarn twisting on the body of the yarn on either side of the middle of the splice. The cross section of this region distinctly shows the fibers of the two yarn strands separately without any intermingling of the fibers, as can be seen in Figure 1 (b).

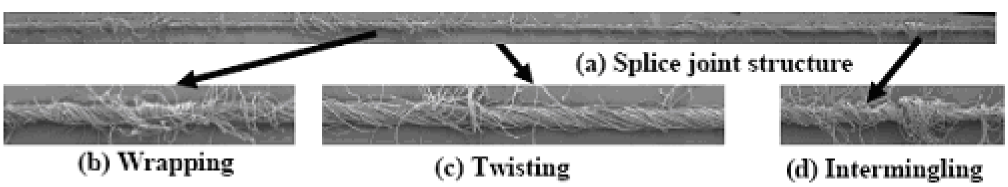

Figure 1. Magnification image of the splice

3. Intermingling: the middle portion of the splice is a region with no distinct order. The fibers from each yarn end intermingle in this splice zone just by tucking.

Referring to Figure 1, it can be seen that wrapping and intermingling contribute the most to the appearance of the splice. The splice appearance is assessed either by simple visual assessment or by comparing it with an image of the standard splice. The textile expert classifies this image visually, either by estimating the degree of wrapping, twisting and integument compared to the un-spliced part, or by comparing it with a standard splice image of the same yarn. This method is time consuming and cost intensive.

It has been proposed to use digital techniques of image processing for assessing yarn structure and detecting yarn faults. Several approaches have appeared in recent years, based on statistical and spectral techniques (e.g. see [5, 6]). On the other hand, detection and classification of spliced yarn joint has been poorly investigated, and only a few papers are available in the scientific literature [7, 8]. In particular, the identification [7] and classification of spliced wool has been presented based on artificial neural networks. In this study, two types of features are used to assess the splice; measurable properties (breaking force, breaking elongation and length of splice) and non-measurable characteristics involving the use of microphotographs of the spliced yarn by a human (leak of proper orientation of the elementary fiber in a splice and intensity of un-spliced yarn ends not joined with the yarn core along the splice length). However, this study also combines the physical and spectral features of the splice. It suffers from the serious drawback that the assessment of the quality of the splice depends on the experience of the person and cannot its use is impractical. For this reason, a new approach for the unsupervised detection and classification of the splice joint is presented in this study.

Thus in this paper an attempt has been made to automatically identify and classify spliced yarn joints. A new classification scheme is devised in which the LBG algorithm is used for clustering the yarn image into two clusters, i.e. yarn section and splice joint section. The segmented joint is classified according to the degree of its similarity to the same non-spliced section of the yarn using the DTW algorithm. The system has been tested using a large set of splice databases, and the results obtained show great promise.

2. System overview

2.1. The proposed system and its application

An initial target application of this study is to design an unsupervised system for detection and classification not only of the splice joint but also the major yarn defects. In this system four key stages are required:(1) to analyze and pre-process the image (image pre-processing), (2) to segment the yarn image into constituent parts (image segmentations), (3) to identify possible objects i.e., splice region and different defects, and finally (4) to analyze the defects (region analysis). The work presented in the remainder of this paper focuses on the segmentation and analysis of the spliced joint. Some works are ongoing on the other parts and further results will be published soon.

2.2 Related tools for splice detection and classification

Smoothness and orientation of individual fibers around a joint are the most important qualities when analyzing the splice joint. In practice, every splice joint exhibits some form of smoothness and fiber orientation. Thus, determination of the degree of smoothness and fiber orientation would be a practical means to detect and classify the splice joint. This can be measured by the degree of intensity and intensity distribution of the gray image. Image segmentation is the process by which yarn and splice regions are accurately proportioned based on the intensity distribution of the gray image. To perform the splice segmentation in this research, the LBG algorithm is used to cluster the spliced yarn into yarn and splice joint segments, by dividing the spliced yarn image into *k* groups for estimating the mean of each group. The segmentation of the spliced yarn is based on this mean. This approach has been chosen for two reasons: (1) a rapid algorithm exists for LBG clustering, (2) it provides unsupervised segmentation of the splice joint, eliminating the need to predefine splice joint features, which are difficult to be generalized for all types of yarns. We test this approach for different *k* values. We conclude that *k=8* yields the best result.

Classification of the splice joint is done by measuring the degree of similarity between the segmented splice and the same non-spliced section of the yarn. The dynamic warp timing (DTW) technique is used for splice classification. DTW is a simple and effective technique for determining the degree of similarity between two different data of different length parameters. In the following section, we present an in-depth discussion of our approach for segmentation and classification based on LBG algorithm and the DTW technique.

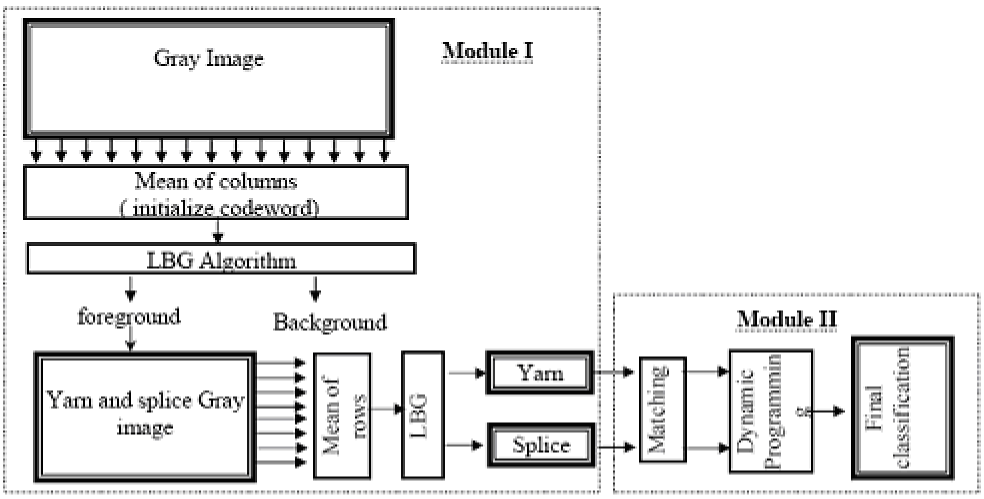

Figure 2. Schematic diagram of the proposed algorithm

3. Detailed algorithm of the system

The proposed system assumes that the information needed to characterize the splice joint can be extracted from the gray level image. Our algorithm consists of two modules, as shown in Figure 2.

3.1. Module I: Segmentation of the spliced area

The analysis of the underlying image statistics reveals statistical differences between foreground and background intensities. A common unsupervised image segmentation algorithm attempts to classify the data into *k* clusters through minimization of the dispersion within each cluster, based on a statistical measure. Clustering is the process of finding natural groupings within a set of data [9]. Several types of clustering algorithms, exist such as K-means, C-means, fuzzy C-means, hierarchical trees etc. [10, 11]. For the purposes of this research, a vector quantization (VQ) method will be used. Specifically, the LBG (Linde, Buzo, and Gray) vector quantization algorithm will be used [12].

The concept of vector quantization is used to represent a data set ***X*** of *m*-dimensional vectors by a set of prototype vectors ***Y,*** such that a total distortion is minimized .

$$X = \left\{ x_i \in R^m \right\},\ i \in \{1, 2, \ldots, n\} \quad (1)$$

$$Y = \left\{ y_j \right\},\ j \in \{1, 2, \ldots, L\},\ L \ll n \quad (2)$$

Where: ***Y*** and $\boldsymbol{y}_j$ are known as a vector quantization codebook and its elements as codewords respectively. The LBG vector quantization algorithm addresses the problem of VQ codebook by iteractively generating the increased codebooks $\boldsymbol{Y}^r$ where:

$$Y^r = \left\{ y_i^{(r)} \right\},\ i \in \left\{1, \ldots, 2^r\right\}_{r = 0, 1, 2, \ldots} \quad (3)$$

We will illustrate how this algorithm works by the following example.

Suppose we have a spliced yarn image (Figure3) in which we want to cluster (or segment) the splice part. Our first task is to segment the image into two classes, that is, foreground (yarn and splice) and background. Secondly, the splice area is segmented from the foreground image. The images we are dealing with are of 8 bits gray intensities. Let a spliced yarn image be

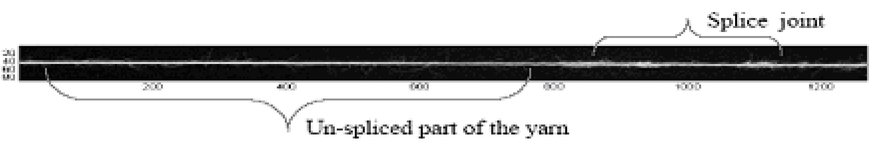

Figure 3. Spliced yarn image

$$X(n, m) = \left\{ x_i \in R^m \right\},\ i = 1, \ldots, n \quad (4)$$

where *n* is the number of rows, and *m* is the number of columns. This image is mapped into two dimensional spaces, as shown in Figure 4(a), where the horizontal axis represents the number of features, and the vertical axis is the gray intensity of pixels from 0 to 255 given by:

$$\boldsymbol{x}_i = \left(x_{i1}, x_{i2}, \ldots\ldots, x_{im} \right),\ i = 1, \ldots, n \quad (5)$$

where x_{ij} is the gray intensity value of pixel $X(i, j)$.

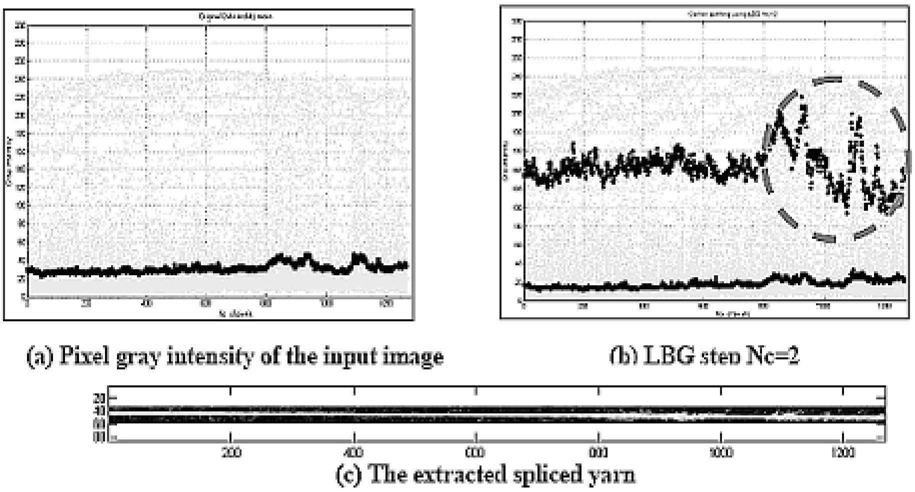

Figure 4. Spliced yarn segmentation
(the black dots represent the value of VQ codebook)

A: Segmentation of the spliced yarn

As we can see in Figure 4(a), the data tends to fall into distinct clusters. The homogeneous portion of the data with the lower pixel intensity represents the background, while the higher intensity portion represents the spliced yarn. We will now apply the LBG vector quantization algorithm to this data, with only 2 codewords for clustering the image into 2 classes; spliced yarn and background. Taking into consideration that the pixel intensity of spliced yarn part is greater than the background, we classify the group of the highest codebook as spliced yarn, and the other group as background. In our example, the group 2 has the highest codewords and has been chosen as the spliced yarn. The clustered spliced yarn is shown in Figure (4-c).

B: Segmentation of the spliced area

In this step, we segment the spliced joint from the spliced yarn image shown in Figure 4 (c), once again using the LBG algorithm. In Figure 4 (b) it can be seen that the VQ code of the spliced yarn (the upper black dots) is almost homogeneous, except for the pixels range from 800 to 1200 marked by the dashed circle. This area represents the splice part of the yarn which we are going to segment. We apply the same methodology as mentioned above for clustering the spliced yarn image into yarn and splice part, i.e. pixels with high intensity values are classified as a splice.

This seems reasonable since the splice area is not smooth compared to the yarn area so that the probability of high intensity distribution in this area may be more than for yarn. The most common difficulty in this step is to determine the right number of codewords. We apply our method using different amounts of codewords, i.e. 2, 4, 8, 16, 32, and 64 codes respectively, and found that the greater the number of codes in the VQ codebook, the better the clusters that are obtained. This can be taken too far however; if we allowed the VQ codebook to increase to more than 8 codewords, misclassification resulted. We thus apply our algorithm using only 8 codewords. In addition we found experimentally that segmentation of the spliced joint based on the highest 2 codewords yields a better result. Following this methodology, we sorted the 8 codewords resulting from the LBG and considered the highest 2 codewords as the spliced joint. The segmented splice is shown in Figure 5.

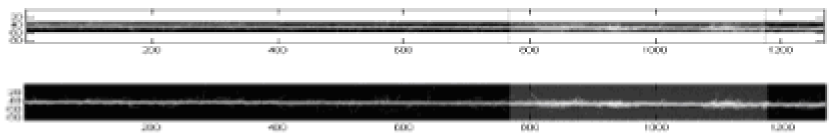

Figure 5. Spliced joint segmentation

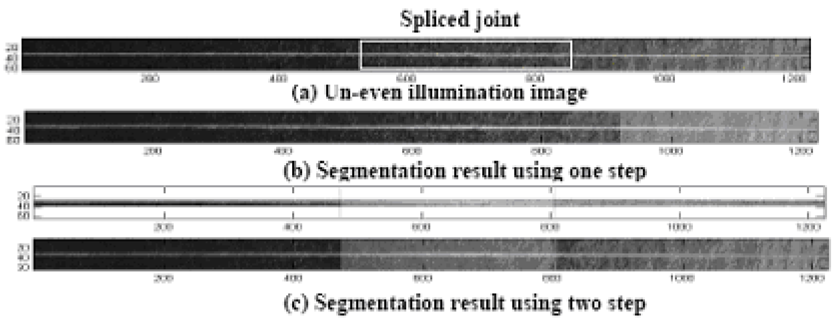

Figure 6. Comparison between one and two step segmentation for un-even illumination image

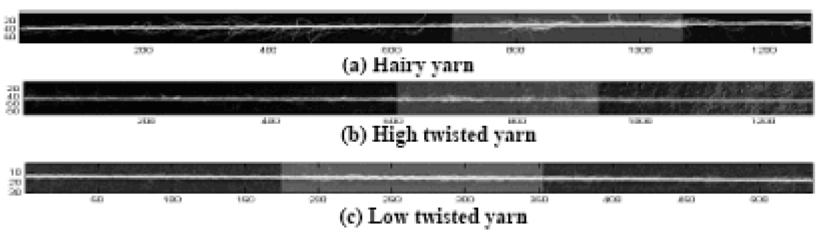

Figure 7. Different types of spliced yarn

The reason for choosing the two-step segmentation is to overcome uneven illumination or shadows in the images. To illustrate that we apply both a one-step and two-step segmentation on the image, as shown in Figure 6(a), where the spliced joint is marked by a white rectangle. The results of both approaches are shown in Figures 6(b), and 6(c) respectively. It can be easily seen that the un-even illumination (the right part of the image) affected the obtained segmentation results, and using two-step approach yields a better result.

3.2. Module II: Unsupervised classification of the splice

A: An overview of the splice classification

The task of splice classification is to categorize each splice area, represented by its feature vectors, into one of three categories; good, medium, or bad. However, it is difficult to find general feature vectors that can represent splice joint properties since they depend on the original yarn. Thus the extracted feature vectors of the splice joint specifications may be used only for each yarn or for a group of similar yarns. Lewandowski & Stanczyk [7] have made the first attempt to describe the splice features. They defined two kinds of appearance features of the splice, the fiber tangling in the place of jointing, and lack of proper orientation of the elementary fibers in a joint. They used standard microphotographs of splice joints with three degrees of categories as a reference, and categorize the splice by comparing it with the reference. However, this method is used for only spliced wool, and it suffers from a serious drawback in that its performance depends on the experience of the people making the judgment. Furthermore it requires extraction of the feature vector of the joint every time a classification is made.

Another way to classify the splice image is to compare it with a prototype image and find the range of similarity between both of them. The prototype or reference image should be representative for different kinds of yarn in order to yield a significant result. For example, Figure 7 shows three kinds of good splice joints for three different yarns. Figure 7(a) shows the extracted splice joint of hairy yarn. Although the joint seems non-uniform, it is classified as good because the original yarn is non-uniform. The other one is for low twisted yarn. It is clear that the two joints have a completely different structure and cannot be compared with the same prototype model. To overcome this problem, we use the same yarn as a reference image and find the degree of similarity between its non-splicing part and the splice joint by using the dynamic time warping (DTW) algorithm. Dynamic time warping is a favored technique for non-linear time alignment [13]. DTW uses dynamic programming to find the optimal sequences of data of different lengths.

B: Main steps in the splice classification using DTW

The design of the automated quality ranking system which we present is based on the criterion that human experts use to inspect splice joints. In the textile industry, experts use a common standard procedure for the examination of the joint. This procedure results in the determination of three different degrees of quality; good, medium, or bad. The experts judge the joint by comparing it with the same yarn, and give their assessment according to the degree of similarity between the joint and same yarn. The most important criterion for comparison is the smoothness along the joint, as well as the proper orientation of individual fibers around the joint. In a bad joint the smoothness is distributed by waves. A well known representation of the waviness is the Fourier transform [14]. We compute the spectrograms of both yarn and splice patterns, that is the magnitude of Short-Time Fourier Transform (STFT) of yarn and splice patterns, and then define a measure of the closeness of the match between splice and yarn spectrograms by computing a matrix comprising all possible matches. The procedure is as follows:

1. Represent *(n,m1)* yarn image and *(n,m2)* splice image by $n \times m1$ and $n \times m2$ dimensional vectors, respectively, assuming both vectors to be ***y*** and ***s***. These vectors are divided into small overlapping segments to which the Hann window function is applied.

$$Hann\ window\ \ w\ (n)=0.5\left(1-cos\left(\frac{2\pi n}{N-1}\right)\right) \quad (6)$$

where:
N represents the width of the Hann window function (we use *N=256*, and 50 % overlapping i.e. number of overlapping = 128) , and *n* is an integer with values $0 \le n \le N-1$.

2. The STFT features of both yarn and splice vectors are calculated by applying the Fast Fourier Transform (FFT) to the product of window function and these vectors as shown in Figure 8. Let , $\boldsymbol{S}\left(\boldsymbol{r},\boldsymbol{p2}\right)$ be the spectrograms of yarn and splice images respectively, where *r* is the spectrogram width , $r=\left(N/2\right)+1$ and *p1* and *p2* are the number of columns of both spectrograms respectively given by:

$$p1=\frac{\left(n\times m1\right)-number\ of\ overlapping}{N\ -number\ of\ overlapping} \quad (7)$$

$$p2=\frac{\left(n\times m2\right)-number\ of\ overlapping}{N\ -number\ of\ overlapping} \quad (8)$$

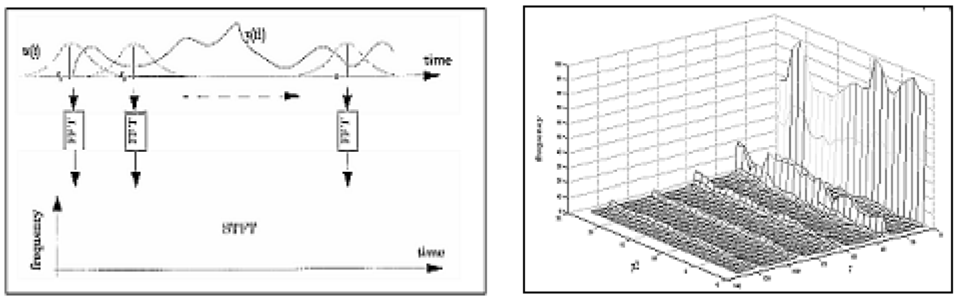

a) b)

Figure 8. (a) STFT, **(b)** An example of a splice spectrogram

3. Construct the local matching matrix ***(MM)*** as the cosine distance between the spectrograms. Every possible mapping from ***S*** to ***Y*** can be represented as a warping path in the matching matrix.

$$MM=\frac{\left|Y^{T}S\right|}{\left|Y\right|\left|S\right|} \quad (9)$$

Where ***MM*** is the cosine distance between vectors of matrices ***Y*** and ***S*** : $-1<MM\ \le 1 \Rightarrow \left|MM\right| \le 1$

4. Construct the cost matrix between yarn and splice spectrogram. Taking into consideration that the aim is to find the lowest matching cost, we calculated the lowest matching cost by the following equation:

$$CM\left(i,j\right)=1-MM\left(i,j\right),1\le i\le p1,1\le j\le p2 \quad (10)$$

5. Using dynamic programming (DP) to find the optimal matching given by the best possible warping path through the cost matrix. i.e. find the lowest-cost path between the opposite corners of the cost matrix. For a cost matrix of length *p1* and *p2* shown in Figure 9 ,a $\left(p1+1\right)\times\left(p2+1\right)$ matrix ***A*** can be constructed by Dynamic Programming given by Eqs .(11)&(12) and the value of ***A(p1+1,p2+1)*** is the accumulated matching cost. The matrix can be constructed from ***A(0,0)***, from top to bottom and left to right

$$A\ (i,j\ )=CM\ \ (i,j\ )+min\begin{Bmatrix}A\ (i-1,j-1\ )\\ A\ (i-1,j\ )\\ A\ (i,j-1\ )\end{Bmatrix} \quad (11)$$

$$\begin{cases}A(0,:)\ =NaN\\ A(:,0)\ =NaN\\ A(1,1)=0\end{cases} \quad (12)$$

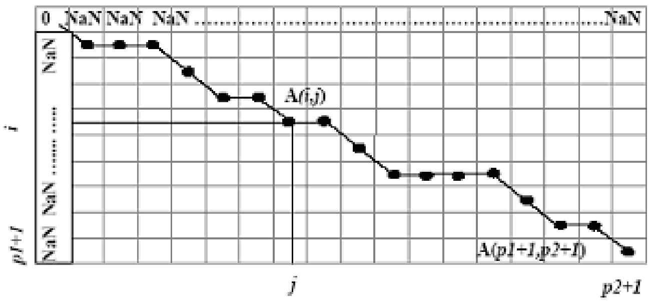

Figure 9. The accumulated cost matrix of the matching cost between yarn and splice

6. According to this least cost, the splice joint could be ranked into one of three categories: good, medium, or bad. The experimental results of the pre-tested data showed that the maximum matching cost between a good splice and the non-spliced part of the same yarn was less than 0.2 (i.e. 80 % matching); while for a medium splice it was less than 0.3 (70% matching); and bad splices were obtained when the highest matching cost was more than 0.3. Consequently, we calculated the accumulated matching cost through the

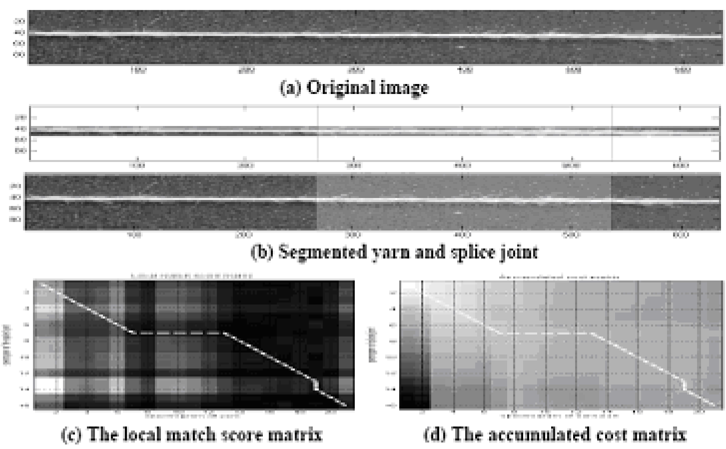

Figure 10 . An example for classification of good image using DTW

matching matrix and our classification fell into one of three categories:

- Good splice joint: for the minimum matching $cost \le 0.2$.
- Medium spliced joint: $0.2 \succ cost \le 0.3$.
- Bad spliced joint: $cost > 0.3$.

Figure 10. shows an examples of splice processes using this technique. As we can see, it is difficult to distinguish between the yarn and the splice joint because the joint is almost as good in appearance. There is a high similarity value(the dark strips between yarn and splice in Figure 10(c)) and the minimum accumulated distance is 0.12. This joint is classified as a good splice

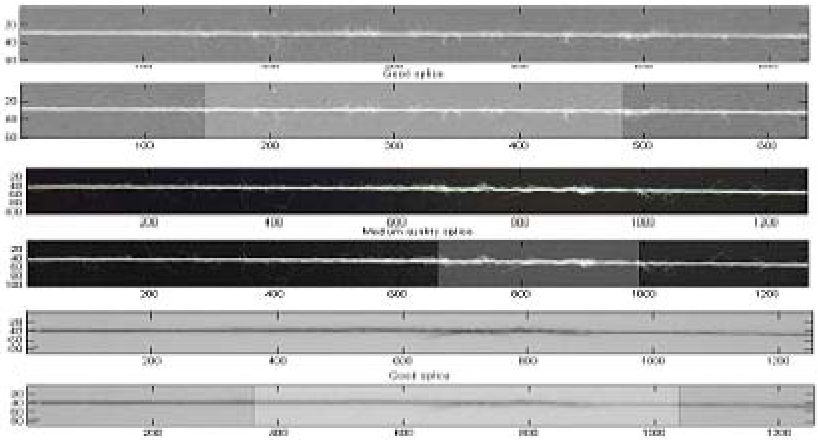

Figure 11. Examples of splice segmentation and classification

4. Experimental design and results

4.1. Experimental data

In order to assess the validity of this method, we performed three types of experiments. The first one uses 120 images (100 × 400 pixels) of 12 groups of yarns containing different grades of splice quality. The images are acquired in working condition and stored without any post processing. In the first phase, the human expert analyzes and ranks the splice joint offline. In the second phase, we apply our algorithm and the results are recorded. The second and third experiments are done by using MURATA database of spliced yarn. This database is used with the approval of the Textile Machinery Division of Murata Machinery. This database consists of two different kinds of classified images, that is, 280 standard images of 14 different spliced yarn.; These images include good spliced joints as well as 1400 images from the daily work and customer claim reports of the MURATA winding research team.

Table 1. Detection Performance

	Experiments		
	1	2	3
Overall detection rate	117/120 97.5 %	272/280 97.1 %	1342/1400 95.8 %

Table 2. Classification Performance

		Experiments		
		1	2	3
Overall classification accuracy		115/120 (95.8 %)	272/280 (97.1 %)	1302/1400 (93 %)
Bad Detection rate		4.1 %	2.8 %	7%
Classification accuracy for each degree of quality	Good	81/82 (98.5%)	272/272 (100 %)	967/1050 (92%)
	Medium	15/18 (83.3 %)	-	217/230 (94.3) %
	Bad	19/20 (95%)	-	118/120 (98.3%)

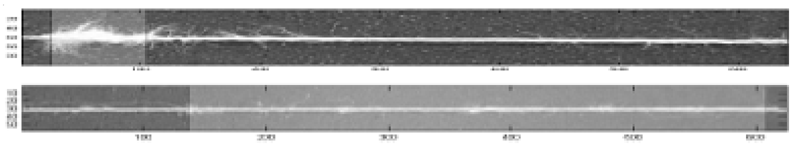

Figure 12 . Some examples of false alarm detections of the spliced joint

4.2. Experimental results

Figures 11 shows examples of the results obtained by the three experiments. The results of the detection and classification of the appearance of the splice joint are shown in Tables 1 and 2, respectively. Analyzing the data in Table 1, we can state that a high detection rate was achieved for the three tests, the highest being for experiment number one. This highest detection rate of these groups of images (experiment 1) could be related to the higher recognizable distance between yarn and splice classes, as it contains different grades of splice joints. The minimum detection rate is recorded for the group of images in experiment 3 because this group contains a number of images in which the yarn itself contains some parts with more defects than the splice joint, yielding the poor detection shown in Figure 12.

Analyzing the data in Table 2, we can state that the highest classification accuracy for the successfully detected joint is achieved using standard images i.e., group number 2, followed by the images of groups 1 and 3 respectively, and that this could be related to the previously mentioned reasons. Moreover, the proposed method could be used to detect and classify splice joints in different illuminations, as shown in Figure 11.

5. Conclusions

This paper has presented a number of image processing techniques applied to spliced yarn images with positive results. This method offers a new approach for the unsupervised classification of spliced joints based on their appearance. The results from the unsupervised LBG splice segmentation were good and constitute an excellent starting point from which a system for segmentation and classification of different yarn faults could be built. Furthermore, it was shown that this classification system of the splice joint based on degree of similarity resulted in a good classification scheme with practical applications. Moreover, this method is more flexible for the detection of spliced joints under different illuminations. Future work will be focused on the detection and classification of different kinds of yarn faults using both static and dynamic images.

Acknowledgements

Murata Machinery, LTD Company supported this project by providing all the database images used. The authors sincerely thank the winding process team for their support and helpful advice and discussions. The paper was originally presented at the Fifth IASTED international conference on Visualization, Imaging, and Image Processing, Spain, August 2006.

References:

1. *Rudolf Luz, Method and apparatus for preparing yarn ends for splicing, USP 4,528,808 7/1985 57/22.*
2. *Koji Deno, Yarn end untwisting device for a pneumatic yarn splicing device, USP 4,494,366 1/1985 57/22.*
3. *Khaled Issa & Rudi Grutz, New technique for optimizing yarn-end preparation on splicer and a method for rating the quality of yarn end. Autex Research Journal, 2005, Vol.5, No.1, pp.1 19.*
4. *Cheng.K.P.S and Lam H.L.I., 'Physical properties of pneumatically spliced cotton ring spun yarn', Textile Res.J.,70,2000,12,1053-1057.*
5. *Cybulska M. Assessing yarn structure with image analysis method. Textile Res. J.69, 1999,05, 369-374.*
6. *Emery, N. B., and Buchanan, D. R., Yarn Package Inspection with Computer Vision and Robotics, Textile Res. J. 58, 605-614 (1988).*
7. *Stanislaw Lewandowski, Tomasz Stanczyck, 'Identification and classification of spliced wool combed yarn joints by artificial neural networks', Fiberes & Textile in Eastern Europe, 2005, Vol.13 No 1.(49), pp. 39-43.*
8. *Lewandowski S., Drobina R., 'Strength and Geometric Sizes of Pneumatically Spliced Combed Wool Ring Spun Yarns', Fibres & Textiles in Eastern Europe, 2004, Vol.12, No 2 (46), pp. 31-37.*
9. *G. B. Coleman and H. C. Andrew, 'Image segmentation by clustering', Proc. IEEE, 67,5, May 1979, 773-785.*
10. *J-H. Wang and C-Y. Peng, "Optimal Clustering Using Neural Networks," IEEE International Conference on Systems, Man, and Cybernetics, Vol. 2, pp. 1625-1630, 1998.*
11. *Likas, A., Vlassis, N., & Verbeek, J. J. (2003). The global k-means clustering algorithm. Pattern Recognition, 36, 451–461.*
12. *Linde, Y., Buzo, A., & Gray, R.M. (1980). An algorithm for vector quantizer design. IEEE Transactions on Communication, COM-28, 84–95.*
13. *Keogh, E., & Pazzani, M. (2000) Scaling up dynamic time warping for datamining applications. In 6th ACM SIGKDD International Conference on Knowledge Discovery and Data Mining. Boston.*
14. *William K. Pratt Digital image processing 3rd ed. (Academic press, New York, 2001) pp. 189-199.*

∇∆